# The low-lying electronic states of MgO

Charles W. Bauschlicher, Jr.* and David W. Schwenke†

*NASA Ames Research Center, Moffett Field, CA 94035*

## Abstract

The low-lying singlet and triplet states of MgO have been studied using a SA-CASCF/IC-MRCI approach using the aug-cc-pV5Z basis set. The spectroscopic constants ($r_e$, $\omega_e$, and $T_e$) are in good agreement with the available experimental data. The computed lifetime for the $B$ state is in excellent agreement with two of the three experimental results. The $d$ state lifetime is in good agreement with experiment, while the computed $D$ state lifetime is about twice as long as experiment.

Keywords: electronic transitions, lifetimes, spectroscopic constants

* Mail Stop 230-3, Thermal Protection Materials Branch, Charles.W.Bauschlicher@nasa.gov

† Mail Stop 258-2, Computational Physics Branch

## I. INTRODUCTION

Magnesium is a common element in silicate rocks, such as those found in stony meteors. Mg atoms are therefore an ablation product of meteor entry, which produces a constant flux of Mg that is deposited in the upper atmosphere, where Mg contributes to the chemistry. The ablation process produces Mg in electronically excited states and Mg atom emission has been observed. In the wake of the entering meteor, these Mg atoms can react with O atoms, also formed in the shock layer, to make electronically exited MgO, which can emit.

Given its contribution to atmospheric chemistry there have been several experimental[1–10] and computational[10–12] studies of MgO. Many features of the spectroscopy of MgO have been determined accurately by experiment; the $r_e$, $\omega_e$, and $T_e$ values of many of the low-lying states are well established. The dipole moment values of the $X$ and $B$ states have been reported[1]. Finally we should note that the dissociation energy of MgO has been of some controversy[13]; in addition to the uncertainty in the measurements, the $X$ state does not dissociate to ground state atoms, which has led to additional confusion.

The lifetimes of the excited states are not well established. The $B^1\Sigma^+$ state $\nu'$=0 lifetime was measured to be 32.7±1.7 ns by Diffenderfer et al.[10], 22.5±1.5 ns by Büsener et al.[1], and 21.5±1.8 ns by Naulin et al.[2]. Naulin et al. noted that their band heads suggested that $J'$ was approximately 70 and this should also apply to the experiments of Diffenderfer et al., while Büsener et al. reported their value as $J'$=1. Thus two experiments, one with $J'$=1 and the other with $J'$ ≈70 support a value of about 22 ns, while one experiment with $J'$ ≈70 favors a higher value.

The calculations of Diffenderfer et al. (24 ns) would seem to support the lower value, while Maatouk et al.[12] computed $J'$=0 lifetime of 33.3 ns, which supports the longer lifetime value. However, Maatouk et al. suggested the experiments with the shorter lifetimes were for $J'$=70, and reported a computed lifetime of 22.0 ns for this $J'$ value. They then suggested their calculations show that both experimental values were correct; the longer lifetime is for $J'$=0 while the shorter lifetime for $J'$=70. This interpretation appears odd because the variation in lifetime with $J'$ reported

by Maatouk et al. seems unreasonably large. In addition to the $B$ state lifetime, experimental lifetimes of the $D^1\Delta$ and $d^3\Delta$ have been reported[2,10].

In this manuscript we reinvestigate MgO with the focus on obtaining accurate transition dipole moments so that precise emission data can be generated for the low-lying states. The computed lifetimes are compared with the measured lifetimes.

## II. METHODS

We are interested in the singlet and triplet states arising from the low-lying states of Mg and O, namely the Mg $^1S_g$ state with the O $^3P_g$, $^1D_g$, and $^1S_g$ states, and the Mg $^3P_u$ state with the O $^3P_g$ state. This gives rise to three $^1\Sigma^+$, two $^1\Sigma^-$, three $^1\Pi$, two $^1\Delta$, one $^3\Sigma^+$, three $^3\Sigma^-$, three $^3\Pi$, and one $^3\Delta$ states. In addition to these states, the previous studies[11,12] have shown an additional low-lying $^3\Sigma^+$ state, so this was added to our study. Our initial procedure was to perform dynamically weighed[14] state-averaged complete active space self-consistent-field (DW-SA-CASSCF) calculations for the singlets and triplets identified above. The Mg $1s$, $2s$, and $2p$ orbitals and the O $1s$ and $2s$ orbitals are treated as inactive. The oxygen $2p$ and $2p'$ and Mg $3s$ and $3p$ orbitals are in the active space. More extensive correlation is included using the internally contracted multi-reference configuration interaction (IC-MRCI) approach[15]. The CASSCF configurations are included in the reference space and the oxygen $2s$ orbital is also correlated in the IC-MRCI calculations. The augmented correlation consistent quintuple zeta (aug-cc-pV5Z) basis[16–19] is used. However, as discussed below, this choice of states does not lead to smooth potentials at the IC-MRCI level. Additional states were added to the DW-SA-CASSCF and IC-MRCI approach until smooth potentials were obtained, at least for the states of most interest to us. The need to add more states was not unexpected as the initial choice of states considered only the low-lying atomic states, but this system is very ionic and states arising from the $Mg^+$+$O^-$ and $Mg^{+2}$ and $O^{-2}$ can become important in the bonding region. The final choice of states is discussed below.

The calculations were performed in $C_{2v}$ symmetry and by averaging all components of the degenerate states, the DW-SA-CASSCF wave functions effectively have $C_{\infty v}$

symmetry. However, the IC-MRCI wave functions only have $C_{2v}$ symmetry, and therefore the $A_1$ and $A_2$ components of the $\Delta$ states are not identical. We study both components and the calculations yield the same $r_e$ and $\omega_e$ values, and the $T_e$ values differ by less than 3 cm$^{-1}$.

We note that our approach is similar to that of Maatouk et al.[12], but we should point out some important differences. Maatouk et al. reported their basis sets as cc-pV5Z, but from the number of functions they report, it is more likely that they used the cc-pCV5Z sets. Since they do not correlate the core electrons, the tight functions they include are not expected to have any significant effect on the results. However, their basis set is missing the diffuse functions, which we include, that will improve the description of $O^-$, therefore our basis set is expected to be superior for MgO. They include the oxygen $2s$ electrons in the CASSCF, while we do not. The addition of the second set of oxygen $2p$ orbitals to the CASSCF is to improve the description of $O^-$ due to $2p$ to $2p'$ excitations. For oxygen the $2s$ to $3d$ excitation with a recouping of the $2p$ electrons is an important atomic correlation effect, which we do not want to compete with the $O^-$ $2p$ to $2p'$ correlation, so we do not include the O $2s$ in the active space, but we do correlate it in the IC-MRCI treatment.

While the Davidson (+Q) correction gives a small overall improvement in the spectroscopic constants ($r_e$, $\omega_e$, and $T_e$) , the shape of the curves at avoided crossing depends on which version, "fixed", "relaxed", or "rotated", of the +Q is used. At some avoided crossings the +Q correction makes the potentials less smooth. On the basis of the small +Q effect and the visual impression that the potentials look more reasonable at the IC-MRCI level than when any of the three version of the +Q correction are applied, we use the IC-MRCI energies without correction.

In the typical approach, the phase of the transition moments is undefined. We avoid this uncertainty as follows. We pick one $r$ value as reference and perform a standard calculation. We perform the CASSCF calculation for the adjacent point and compute the diabatic orbitals. This makes the orbitals at the second point as similar as possible to those at the first, or reference point. The reference orbitals are orthogonalized using the Gram-Schmidt procedure at the displaced geometry and the overlap between the two sets of orbitals is computed to confirm that the overlap is

larger than 0.5 for analogous pairs of orbitals. We note that while we use diabatic orbitals, we are not performing diabatic calculations. After performing the IC-MRCI, we compute the overlap between the CI vectors for these two points. Since the orbitals are similar and have the same phase, the overlap of the CI vectors allows the phase of the transition moments to be made consistent. We should note that one cannot use a single point as reference for the entire curve since the orbitals change too much for points that differ significantly in $r$ value. So we proceed stepwise and use the previous $r$ value as reference. Overall this procedure works well, but we did find for some choices for the number of states included in the calculation, that for some of the upper states at specific $r$ values, problems arose. This occured because the overlap of the CI wave functions was very small due to an avoided crossing, which dramatically changes its character at this point. For these few crossing points, our automatic determination of the phase did not work and we adjusted the overlap by hand to make the transition moment curves smooth. We should note that this is not as arbitrary as it might initially seem as there are several moments for each state and this phase adjustment made all of the moments smooth. In addition, this problem tends to happen for the higher lying states, so adding more states not only improves the shape of the potentials, it eliminates the phase problems for the states of most interest.

A series of calibration calculations are performed using the coupled cluster singles and doubles approach[23], including the effect of connected triples determined using perturbation theory[24], CCSD(T). For the open-shell systems the partial spin restricted, RCCSD(T), approach[25] is used. Two series are used; in the first, only the valence electrons are correlated and in the second, all electrons except the Mg $1s$ are correlated. These calculations use the aug-cc-pCV5Z set[26,27]. This basis set starts from the aug-cc-pV5Z sets and adds tight functions for the core correlation and makes the Mg $s$ contraction more flexible. It should produce valence results very similar to the aug-cc-pV5Z, but is also suitable for correlation of the inner shell electrons. The importance of scalar relativistic effects were tested in the CCSD(T) calculations using the Douglas-Kroll-Hess approach[29] and they were found to be very small, so were not included in the reported calculations. All calculations are preformed using

MOLPRO[15,20–22,25].

The best way to compute a very accurate $D_e$ value is to minimize the differential correlation effects. For MgO, which has a very large ionic component to the bonding, one can dissociate to $Mg^+$ and $O^-$ and then correct to the ground state asymptote using the experimental ionization potential (IP) of Mg and electron affinity (EA) of O. This approach can be used for the $a^3\Pi$ state as it is well described by a single configuration and the $T_e$ is well known. Thus our first approach to compute $D_e$ uses

$$D_e = E(\mathrm{MgO}\ ^3\Pi) - E(\mathrm{Mg}^+) - E(\mathrm{O}^-) - IP(\mathrm{Mg}) + EA(\mathrm{O}) + T_e(X-a), \qquad (1)$$

where the compute energies, $E$, are combined with the experimental IP, EA, and $T_e$ values. The $X^1\Sigma^+$ state has more multi-reference character as measured by the T1 diagnostic[28] (the Euclidian norm of the vector of $t_1$ amplitudes divided by the square root of the number of electrons correlated), probably arising from the $Mg^{2+}O^{2-}$ character, and therefore has a sizable differential correlation effect. We use the $X^1\Sigma^+$ state to help assess the accuracy of our approach. The $D_e$ for this state is computed as

$$D_e = E(\mathrm{MgO}\ ^1\Sigma^+) - E(\mathrm{Mg}^+) - E(\mathrm{O}^-) - IP(\mathrm{Mg}) + EA(\mathrm{O}). \qquad (2)$$

The vibrational energy levels are computed using the approach of Tobin and Hinge[30]. The potentials are fit to spline functions and with a centrifugal potential added for $J \neq 0$. The reported $\omega_e$ values are determined by a $1/r$ fit to the three points nearest the minima. For the low-lying states these results are very similar to the results obtained by fitting the four lowest vibrational levels to $\omega_e$, $\omega_e x_e$, and $\omega_e y_e$. For the upper states, the curve crossings and double well potentials means that the two approaches can differ significantly. The lifetimes are evaluated using the computed potentials and transition moments. When the $T_e$ is known from experiment, the computed potentials are shifted to match experiment. The maximum shift was 544 $\mathrm{cm}^{-1}$.

## III. RESULTS AND DISCUSSION

As we noted in the methods section, it was sometime necessary to include more states in the CASSCF and IC-MRCI procedure than originally planned based on specific atomic asymptotes and/or previous results. We illustrate this using the $^3\Pi$ states. Our first calculations included one $^3\Sigma^+$, three $^3\Sigma^-$, three $^3\Pi$, and one $^3\Delta$ states based only on the atomic asymptotes. While the $^3\Sigma^+$, $^3\Sigma^-$, and $^3\Delta$ states appeared quite reasonable, the third $^3\Pi$ state had an unreasonable shape, see Fig. 1. Adding a fourth $^3\Pi$ state to the CASSCF and IC-MRCI improved the third $^3\Pi$ state, but the fourth state looked strange. Including the fifth $^3\Pi$ state resulted in five states that look very reasonable, see Fig. 1. There are only small changes in the $(3)^3\Pi$ state when the fifth state is added. Since the $(4)^3\Pi$ state is similar in energy to the $(3)^3\Pi$, the final calculation included five $^3\Pi$ states. We note that Maatouk et al. plotted their three $^3\Pi$ states and the third state showed a clear hump, which is not present in our curves. This is probably a result of our inclusion of two additional $^3\Pi$ states in the CASSCF procedure.

Our procedure was to perform a calculation including a preliminary estimate for the number of states of interest, then to add one state in each symmetry and repeat the calculations. If the extra state did not affect the states of interest, it was removed. In this way, we determined the number of states to include in the averaging procedure.

The triplet and singlet states are shown in Figures 2 and 3. Thirty-one points between 1.2 and 10 Å were computed for the triplet states. For the singlet states, the point at 1.2 Å was excluded due to convergence problems. These final DW-SA-CASSCF/IC-MRCI calculations included three $^3\Sigma^+$, three $^3\Sigma^-$, five $^3\Pi$, and one $^3\Delta$ states in the triplet study and five $^1\Sigma^+$, two $^1\Sigma^-$, four $^1\Pi$, and two $^1\Delta$ states in the singlet study. We note that our $E^1\Sigma^+$ state shows a smaller hump than that of Maatouk et al.; as for the $^3\Pi$ states, this is probably a result of our including more $^1\Sigma^+$ states in the SA-CASSCF procedure.

The spectroscopic constants are summarized in Table I along with experiment[5,7–9,32]. Before comparing with experiment, we should note that our results are similar to those reported for Maatouk et al.; it appears that the different

basis sets and different numbers of states included in the SA-CASSCF/IC-MRCI procedure did not have a significant effect on the potentials near equilibrium for the states studied. However, on the basis of the lifetimes reported below, the differences in treatment did affect the transition moments.

Before discussing the IC-MRCI results with experiment, we will compare our IC-MRCI and CCSD(T) results for the $X^1\Sigma^+$ and $a^3\Pi$ states, given at the bottom of Table I, since this will give some insight into errors associated with neglecting the core correlation in the IC-MRCI calculations. These calculations will also be used to obtain our best estimate for the $D_e$ value.

The CCSD(T) valence treatment of the $a^3\Pi$ state is in good agreement with the IC-MRCI results, while for the $X^1\Sigma^+$ state the CCSD(T) $r_e$ and $\omega_e$ values are shorter and larger, respectively, than the IC-MRCI results. In fact, the CCSD(T) $\omega_e$ value is larger than experiment. We suspect this is due to the multi reference character that is underestimated in the CCSD(T) approach. However, both states are sufficiently well described that the CCSD(T) approach can be used to assess the importance of the inner shell correlation. A comparison of the valence and core plus valence results shows that inner shell correlation for the $X^1\Sigma^+$ and $a^3\Pi$ states reduces $r_e$ by about 0.014 and 0.013 Å and increases $\omega_e$ by 19 and 5 cm$^{-1}$, respectively. It also increases $T_e$ by 340 cm$^{-1}$. On this basis we speculate that much of the difference between IC-MRCI and experiment arises from neglecting the inner shell correlation in our CASSCF/IC-MRCI calculations. We should note however that some of the error in the $T_e$ values also arise from errors in the asymptotic separations, for example at the IC-MRCI level the $X^1\Sigma^+$-$a^3\Pi$ separation at 10 Å is 180 cm$^{-1}$ larger than the correct separation between these two states, namely the O $^3P_g - ^1D_g$ separation. If this error in the asymptotic separation carries over to the $T_e$ value, this would reduce the error in $T_e$ by an additional 180 cm$^{-1}$. Since our main goal is the spectroscopy of many of the low-lying states, we accept this level of accuracy.

The computed $D_e$ values are summarized in Table II. We first note that using the $a^3\Pi$ state (i.e. eq 1) yields very similar values at the SCF and CCSD(T) levels for the valence and core+valence treatments. That is, there is a very small effect of electron correlation on the $D_e$. Using the $X^1\Sigma^+$ state (eq 2) has a correlation

effect that is essentially equal to the entire $D_e$ value. However, despite this large correlation effect, the best value from the CCSD(T) with core correlation is only 0.03 eV smaller than that obtained using the $a^3\Pi$ state. We should also point out that Prascher et al.[19] performed analogous calculations with no experimental input, by dissociating to ground state atoms and found results very similar to our values. This agreement between the different methods for computing $D_e$, combined with the very small correlation contribution to the $D_e$ for $a^3\Pi$ approach, gives us confidence in our $D_e$, which we suspect is accurate to about $\pm$0.1 eV. Our current estimate (2.7$\pm$0.1 eV) is in good agreement with our previous estimate[13] of 2.65$\pm$0.16 eV. We stress that this is for dissociation to the Mg $^1S_g$ and O $^3P_g$ asymptote. The $D_e$ value for the $X^1\Sigma^+$ dissociating to the asymptote to which it correlates is 4.65 eV. This is significantly larger than the value deduced by Reddy et al.[31] (3.674$\pm$0.075 eV) by extrapolating the ground state potential to dissociation.

Returning to the IC-MRCI results in Table I, our computed $r_e$ values tend to be slightly longer than experiment by 0.01-0.02 Å. On the basis of the CCSD(T) calibrations, this is attributed to the neglect of core correlation. The computed $\omega_e$ values are in good agreement with experiment, and are, in general, smaller than experiment, as expected from the CCSD(T) calibration. The computed $T_e$ values are in good agreement with experiment. In most cases, the computed values are too small, consistent with the difficulty in describing the $X^1\Sigma^+$ state with its $Mg^{+2}O^{-2}$ character and the neglect of core correlation. The computed $X$ and $B$ state dipole moments for $\nu$=0 are 5.99 and 5.72 D, respectively, which are in good agreement with the experimental values of 6.2$\pm$0.6 and 5.94$\pm$0.24 D measured by Büsenet et al.[1].

The computed transition moments are shown in Figure 4 and the computed lifetimes are given in Table III. Our computed lifetime for the $B$ state is mostly determined by decay to the $X$ state. We have a very slow decrease in lifetime with increasing $\nu'$, this was also observed in the calculations of Maatouk et al.[12] and in the experiments of Naulin et al.[2] Our value is in good agreement with the calculations of Diffenderfer et al.[10] and the experiments of Naulin et al.[2] and those of Büsenet et al.[1], but smaller than the calculations of Maatouk et al. and the experiment of Diffenderfer et al. As noted in the introduction Maatouk et al. attributed the difference in

experimental values to the $J'$ values, namely $J'$=0 for the longer experimental value and $J'$=70 for the shorter experiments. Unlike Maatouk et al., our computed lifetime for $J'$=70 is only slightly smaller than that for $J'$=0, 21.7 vs. 22.1 ns. This small difference is consistent with the very similar values for the experiments of Naulin et al. ($J'$=70) and Büsenet et al. ($J'$=1). Therefore we do not believe that the difference between the experimental values can be ascribed to a difference in $J'$. We note that in their Table IV caption they state that they are computing the delay of all $J'$ levels to $\nu''$=0 J''=0. If we ignore the $\Delta J$=±1 selection rule for $^1\Sigma^+ - {}^1\Sigma^+$ transitions and evaluate the $\nu'$=0 lifetime allowing the $J'$=70 level to decay to the $J''$=0 levels, we obtain a lifetime of 16.8 ns, which is shorter than the correctly computed value. Thus we believe that the table caption of Maatouk et al. is correct and that they ignored the $\Delta J$=±1 selection when they determined the lifetime of $J'$=70.

In addition to the $B$ state, we evaluate the lifetimes of the $D^1\Delta$, $d^3\Delta$, $C^1\Sigma^-$, and $c^3\Sigma^+$ states. We find these states have very similar lifetimes, which are determined, or essentially determined, by the decay to the lowest Π state of the same spin, namely the $A^1\Pi$ and $a^3\Pi$ states. For the $D$, $d$, $C$, and $c$ states, 90% of the wave function is described by the occupation $...5\sigma^2 6\sigma^2 2\pi^3 3\pi^1$, while the $A^1\Pi$ and $a^3\Pi$ states are both described by $...5\sigma^2 6\sigma^2 7\sigma^1 2\pi^3$. That is, all of these transitions correspond to a $3\pi \rightarrow 7\sigma$ transition, and not surprisingly they have similar lifetimes. Our computed $d$ state lifetime is in excellent agreement with experiment of Naulin et al. and good agreement with that of Diffenderfer et al. Our compute lifetime for the $D$ state however, is 17% longer than that of the $d$ state, while the experiments of Naulin et al. show the $D$ state to have about half the lifetime of the $d$ state. Given the excellent agreement between our work and that of Naulin for the $B$ and $d$ state, we find the difference for the $D$ state somewhat unexpected. However we should note that lifetime of the $D$ state is close to the temporal width of the laser pulse and hence there could be some additional uncertainty in the experimental value. Another experiment for the $D$ state lifetime would be welcomed.

## IV. CONCLUSIONS

Thirteen singlet and twelve triplet states of MgO have been studied using the SA-CASCF/IC-MRCI approach using the aug-cc-pV5Z basis set. The computed $r_e$, $\omega_e$, and $T_e$ values are in good agreement with the available experimental data. The computed lifetime of the $B^1\Sigma^+$ state of 22.1 ns is in good agreement with the computed value of Diffenderfer et al.[10] (24 ns) and two of the experiments[1,2] that yielded values of 21.5 and 22.5 ns, We suggest that the values of 32.7 and 33.3 ns measured[10] and computed[12] are too long. Our computed lifetime (8.6 ns) for the $d$ state is in good agreement with experiment[2,10] 11.8±0.5 and 7.8±1.8 ns, but our $D$ state lifetime (10.1 ns) is longer than determined in experiment[2], 4.3±1.0 ns. Given the agreement for the $B$ and $d$ states and the similar character for the $D$ and $d$ states and the $A$ and $a$ states, we do not understand the origin of the difference in $D$ and $d$ state lifetimes found in experiment.

## V. ACKNOWLEDGMENTS

This work was funded by NASA.

---

[1] H. Büsener, F. Heinrich, A. Hese, Chem. Phys. 112 (1987) 139.

[2] C. Naulin, M. Costes, Z. Moudden, G. Dorthe, Chem. Phys. Lett 178 (1991) 325.

[3] E. Kagi, K. Kawaguchi, J. Molec. Struct. 795 (2006) 179.

[4] T. Ikeda, N.B. Wong, D.O. Harris, R. W. Field, J. Molec. Spectrosc. 68 (1977) 452.

[5] D. Bellert, K. L. Burns, N.-T. Van-Oanh, J. Wang, W.H. Breckenridge, Chem. Phys. Lett. 381 (2003) 725.

[6] B. Bourguignon, J. McCombie, J. Rostas, Chem. Phys. Lett. 113 (1985) 323.

[7] B. Bourguignon, J. Rostas, J. Molec. Spectrosc. 146 (1991) 437.

[8] P.C.F. IP, K.J. Cross, R.W. Field, J. Rostas, B. Bourguignon, J. McCombie, J. Molec. Spectrosc. 146 (1991) 409.

[9] J.H. Kim, X. Li, L.-S. Wang, H.L. de Clercq, C.A. Fancher, O.C. Thomas, K. H. Bowen, J. Phys. Chem. A 105 (2001) 5709.

[10] R.N. Diffenderfer, D.R. Yarkony, P.J. Dagdigian, J. Quant. Spectrosc. Radiat. Transfer 29 (1983) 329.

[11] H. Thümmel, R. Klotz and S. D. Peyerimhoff, Chem. Phys. 129 (1989) 417.

[12] A. Maatouk, A. Ben Houria, O. Yazidi, N Jaidane, M. Hochlaf, J. Chem. Phys. 133 (2010) 144302.

[13] C. W. Bauschlicher, B. H. Lengsfield, and B. Liu, J. Chem. Phys. 77 (1982) 4084.

[14] M.P. Deskevich, D.J. Nesbitt, H.-J. Werner, J. Chem. Phys. 120 (2004) 7281.

[15] H.-J. Werner, P.J. Knowles, J. Chem. Phys. 89 (1988) 5803; P.J. Knowles, H.-J. Werner, Chem. Phys. Lett. 145 (1988) 514.

[16] T. H. Dunning, J. Chem. Phys. 90 (1989)1007-1023.

[17] R.A. Kendall, T.H. Dunning, R.J. Harrison, J. Chem. Phys. 96 (1992) 6796-6806.

[18] D.E. Woon, T. H. Dunning, J. Chem. Phys. 98 (1993) 1358-71.

[19] B.P. Prascher, D.E. Woon, K.A. Peterson, T.H. Dunning, A.K. Wilson, Theor. Chem. Acc. 128 ( 2011) 69-82.

[20] MOLPRO, version 2010.1, a package of ab initio programs, H.-J. Werner, P. J. Knowles, F. R. Manby, M. Schütz, P. Celani, G. Knizia, T. Korona, R. Lindh, A. Mitrushenkov, G. Rauhut, T. B. Adler, R. D. Amos, A. Bernhardsson, A. Berning, D. L. Cooper, M. J. O. Deegan, A. J. Dobbyn, F. Eckert, E. Goll, C. Hampel, A. Hesselmann, G. Hetzer, T. Hrenar, G. Jansen, C. Köppl, Y. Liu, A. W. Lloyd, R. A. Mata, A. J. May, S. J. McNicholas, W. Meyer, M. E. Mura, A. Nicklass, P. Palmieri, K. Pflüger, R. Pitzer, M. Reiher, T. Shiozaki, H. Stoll, A. J. Stone, R. Tarroni, T. Thorsteinsson, M. Wang, A. Wolf, see http://www.molpro.net.

[21] R. Lindh, U. Ryu, B. Liu, J. Chem. Phys. 95 (1991) 5889.

[22] P. J. Knowles, H.-J. Werner, Chem. Phys. Lett. 115 (1985) 259.

[23] R. J. Bartlett, Annu. Rev. Phys. Chem. 32 (1981) 359.

[24] K. Raghavachari, G.W. Trucks, J.A. Pople, M.A. Head-Gordon, Chem. Phys. Lett. 157 (1989) 479.

[25] P.J. Knowles, C. Hampel, H.-J. Werner, J. Chem. Phys. 99 (1993) 5219 (see also erratum,

J. Chem. Phys., 112 (2000) 3106)

[26] D.E. Woon,T.H. Dunning, J. Chem. Phys. 103 (1995) 4572.

[27] K.A. Peterson,T.H. Dunning, J. Chem. Phys. 117 (2002) 10548.

[28] T. J. Lee, P. R. Taylor, Int. J. Quantum Chem. Symp. 23, 36 (1989) 199-207.

[29] A. Wolf, M. Reiher, B. A. Hess, J. Chem. Phys. 117 (2002) 9215.

[30] F.L. Tobin, J. Hinze, J. Chem. Phys. 63 (1975) 1034.

[31] R.R. Reddy, Y. Nazeer Ahammed, K. Rama Gopal, P. Abdul Azeem, T.V.R. Rao J. Quantitative Spectrosc.Radiative Transfer 66 (2000) 501

[32] K.P. Huber, G, Herzberg, 1979 "Molecular Spectra and Molecular Structure: IV. Constants of Diatomic Molecules," Van Nostrand Reinhold Company.

TABLE I: Summary of spectroscopic constants.

| State | $r_e$(Å) | | $\omega_e$(cm$^{-1}$) | | $T_e$(cm$^{-1}$) | |
|---|---|---|---|---|---|---|
| | IC-MRCI | Exp[a] | IC-MRCI | Exp[a] | IC-MRCI | Exp[a] |
| $(5)^1\Sigma^+$ | 1.962 | | 1658.4 | | 51 730 | |
| $(4)^1\Sigma^+$ | 1.724 | | 864.3 | | 47 293 | |
| $(2)^1\Sigma^-$ | | | repulsive | | | |
| $(3)^3\Sigma^-$ | | | repulsive | | | |
| $(2)^1\Delta$ | | | repulsive | | | |
| $(5)^3\Pi$ | 2.196 | | 701.0 | | 45 394 | |
| $(3)^3\Sigma^+$ | 1.769 | | 716.1 | | 45 200 | |
| $(4)^1\Pi$ | 2.189 | | 1014.8 | | 45 117 | |
| $(4)^3\Pi$ | 1.960 | | 878.9 | | 39 470 | |
| $E^1\Sigma^+$ | 1.826 | [1.829] | 728.7 | [705] | 38 964 | 37 722 |
| $G^1\Pi$ | 1.854 | [1.834] | 686.6 | | 38 887 | 40 260 |
| $(3)^3\Pi$ | 1.864 | | 636.1 | | 37 681 | |
| $F^1\Pi$[b] | 1.782 | 1.766 | 718.6 | 705 | 36 521 | 37 919 |
| $(2)^3\Pi$ | | | repulsive | | | |
| $(2)^3\Sigma^-$ | 2.019 | | 802.4 | | 31 189 | |
| $C^1\Sigma^-$ | 1.886 | 1.872 | 618.7 | 632.4 | 28 903 | 30 081 |
| $D^1\Delta$ | 1.885 | 1.871 | 626.9 | 632.5 | 28 643 | 29 852 |
| $(1)^3\Sigma^-$ | | | repulsive | | | |
| $d^3\Delta$[c] | 1.877 | 1.871 | 649.8 | 655.2 | 28 381 | 29 466 |
| $c^3\Sigma^+$ | 1.869 | | 664.3 | | 27 352 | |
| $B^1\Sigma^+$ | 1.757 | 1.737 | 803.7 | 824.0 | 19 439 | 19 984 |
| $b^3\Sigma^+$[d] | 1.808 | 1.791 | 674.4 | ≈670 | 7 802 | 8 437 |
| $A^1\Pi$ | 1.879 | 1.864 | 660.0 | 664.4 | 2 811 | 3 563 |
| $a^3\Pi$[e] | 1.884 | 1.868 | 643.7 | 650.2 | 1 932 | 2 621 |
| $X^1\Sigma^+$ | 1.769 | 1.749 | 768.6 | 785.0 | 0 | 0 |
| CCSD(T) valence | | | | | | |
| $a^3\Pi$ | 1.883 | | 647.4 | | 2030 | |
| $X$ | 1.753 | | 798.0 | | | |
| CCSD(T) core+valence | | | | | | |
| $a^3\Pi$ | 1.870 | | 652.5 | | 2370 | |
| $X$ | 1.739 | | 817.0 | | | |

[a] Huber and Herzberg[32], unless otherwise noted.

[b] Bellert et al.[5]

[c] Bourguignon, and Rostas[7]

[d] Kim et al.[9]. Note their $T_0$ was converted to $T_e$ using our computed $\omega_e$ values.

[e] Ip et al.[8]

TABLE II: Calculation of $D_e$ for the $X$ state with respect to the Mg $^1S_g$+O $^3P_g$ asymptote

.

| level of theory | Eq 1 | Eq 2 | Prascher et al.[19a] |
|---|---|---|---|
| SCF | 2.73 | −0.03 | |
| CCSD(T) valence | 2.66 | 2.58 | 2.65 |
| CCSD(T) core+valence | 2.71 | 2.68 | 2.65 |

[a] Computed to ground state atoms with no experimental data used. The aug-cc-pV5Z and aug-cc-pCV5Z results are given.

TABLE III: Summary of lifetimes, in ns, for selected excited states of MgO.

| level | State | | | | | | |
|---|---|---|---|---|---|---|---|
| $\nu'$ | $B^a$ | | | $D$ | $d$ | $C$ | $c$ |
| | Total[a] | $B-X$ | $B-A$ | | | | |
| Theory | | | | | | | |
| | | | Present work | | | | |
| 0 | 22.1 | 28.7 | 95.5 | 10.1 | 8.6 | 9.7 | 9.6 |
| 1 | 21.9 | 29.2 | 87.0 | 10.3 | 8.7 | 9.9 | 9.7 |
| 2 | 21.7 | 29.9 | 79.8 | 10.4 | 8.8 | 10.1 | 9.7 |
| 3 | 21.6 | 30.5 | 73.8 | 10.6 | 8.9 | 10.3 | 9.8 |
| 4 | 21.4 | 31.1 | 68.7 | 10.8 | 9.0 | 10.5 | 9.8 |
| | | | Diffenderfer et al.[10] | | | | |
| 0 | 24 | | | | | | |
| | | | Maatouk et al.[12] | | | | |
| 0 | 33.3 | | | | | | |
| 1 | 33.1 | | | | | | |
| 2 | 33.0 | | | | | | |
| Experiment | | | | | | | |
| | | | Naulin et al.[2] | | | | |
| 0 | 21.5±1.8 | | | 4.3±1.0 | 7.8±1.8 | | |
| 1 | 21.9±2.1 | | | | | | |
| 2 | 21.7±2.0 | | | | | | |
| 3 | 21.5±3.2 | | | | | | |
| | | | Diffenderfer et al.[10] | | | | |
| 0 | 32.7±1.7 | | | 11.8±0.5 | | | |
| | | | Büsener et al.[1] | | | | |
| 0 | 22.5±1.5 | | | | | | |

[a] Total is lifetime of the $B$ state, $B-X$ and $B-A$ are the lifetimes computed assuming only $B-X$ and $B-A$ emission occurs.

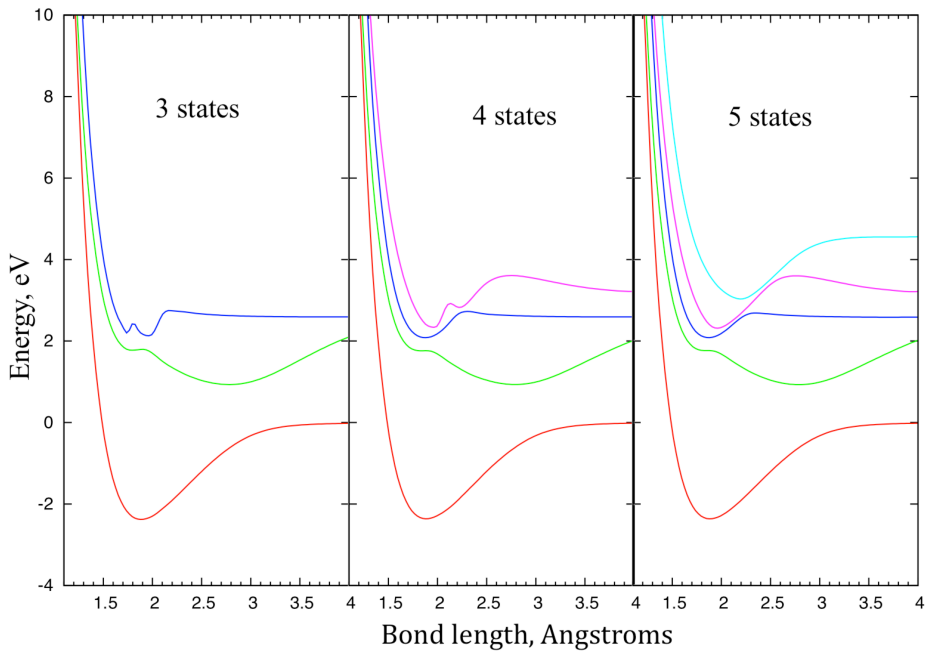


FIG. 1: The computed IC-MRCI potential curves for various numbers of $^3\Pi$ states.

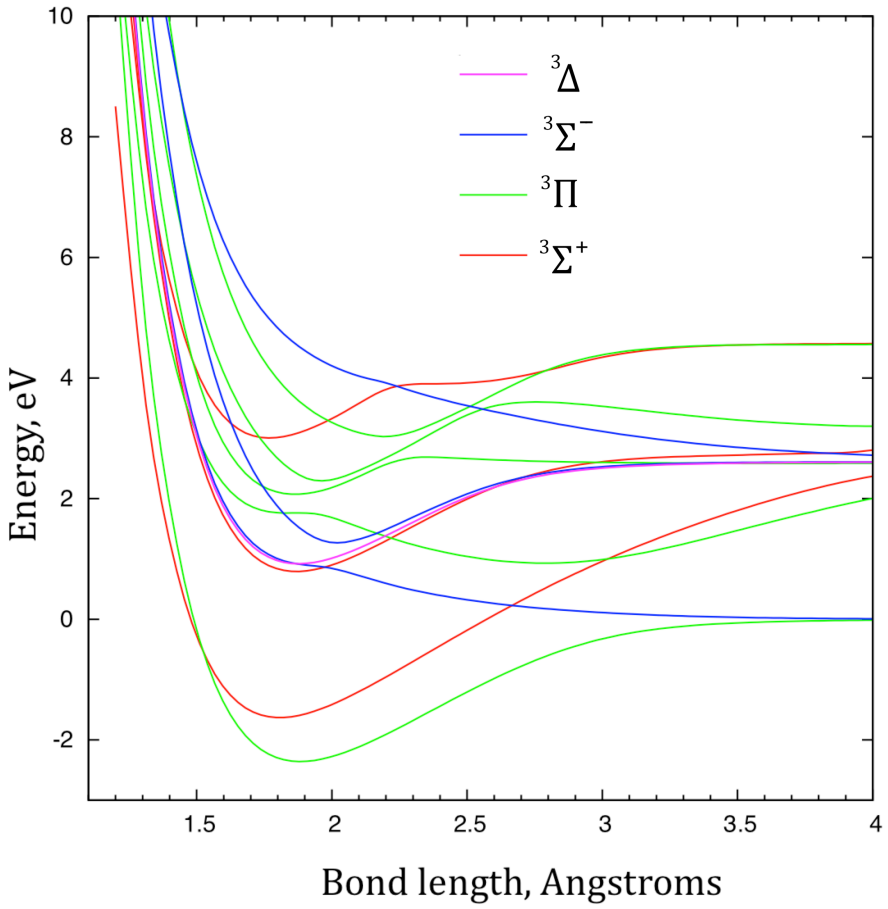


FIG. 2: The computed IC-MRCI potential curves for the triplet states.

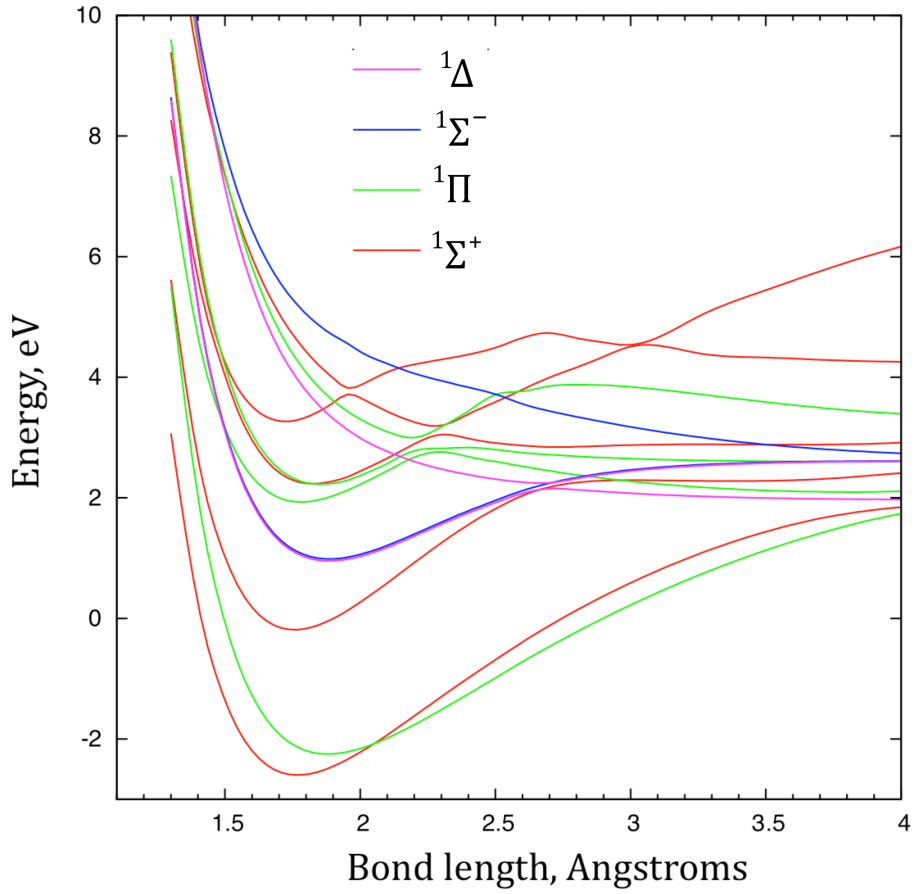


FIG. 3: The computed IC-MRCI potential curves for the singlet states. Note that the $C^1\Sigma^-$ and $D^1\Delta$ states are essentially degerate on this scale and therefore very difficult to separate.

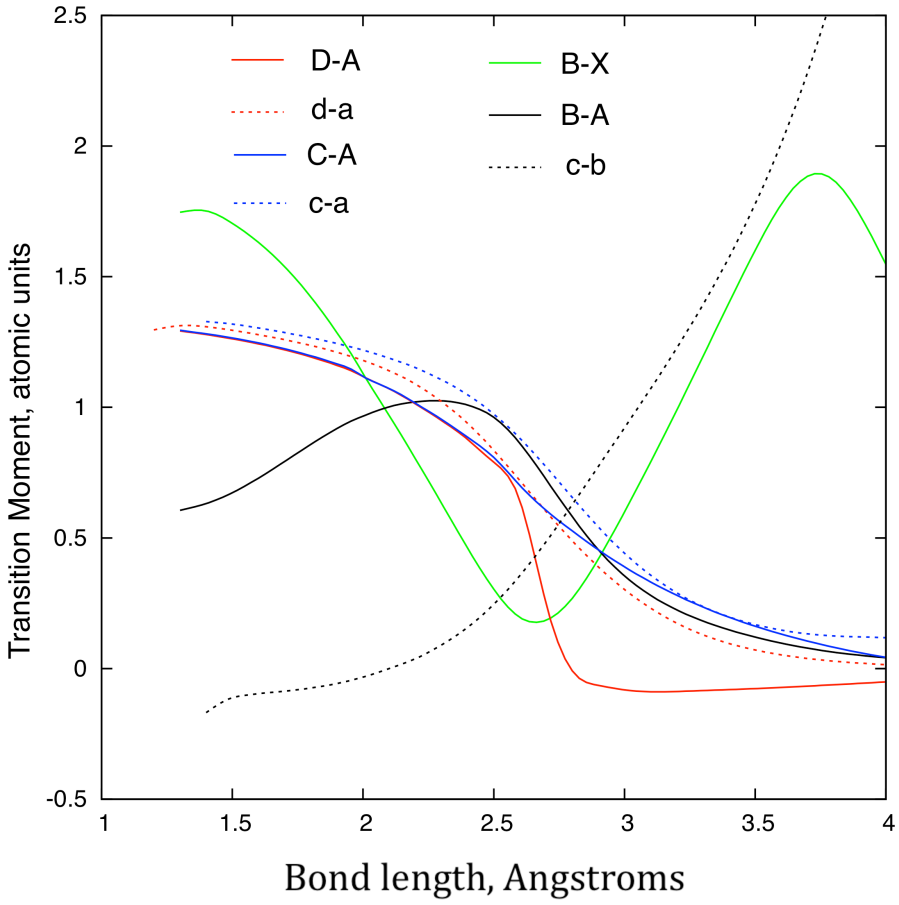


FIG. 4: The computed IC-MRCI transition moment curves for the transitions used to compute the lifetimes in Table III. Note the $D-A$ and $d-a$ moments are the cartesian moment $<\Pi_x|y|\Delta_{xy}>$, where $\sqrt{2}<\Pi_x|y|\Delta_{xy}>=<\Pi|\frac{(x+iy)}{\sqrt{2}}|\Delta>$